Biopolymeric Hydrogel as an Eco-Friendly Soil Amendment for Water Conservation and Sustainable Agricultural Applications

Divya S[1], Chandrika S Tantry[1], Dona Molly Chandy[1], Ellen Ruth Nyirenda[1], Shifali Shetty[1], Zishan Shaikh[1], Shobitha A Rao[1], Manjunatha Bukkambudhi Krishnaswamy[2], Mahanthesh Kumar G T[3], Vidya Shimoga Muddappa[1]*[*]

Abstract

Water scarcity is a major challenge affecting sustainable agricultural production and necessitates the development of biodegradable soil conditioners capable of reducing irrigation demand. In this study, a quaternary polymer composite hydrogel (SLGC) composed of sodium alginate (SA), bacterial cellulose (BC), guar gum (GG), and locust bean gum (LBG) was developed using Ca^{2+}-mediated ionotropic gelation. The optimised formulation (2% SA, 0.4% GG, 0.4% LBG, 0.2% BC, and 4% $CaCl_2$) was characterised using FTIR, SEM, and gravimetric analyses. The hydrogel exhibited a swelling capacity of 450%, water-holding capacity of 82%, water retention of approximately 79%, and re-swelling capacity of 90% after repeated dehydration–rehydration cycles. Pot and germination studies demonstrated improved moisture retention and plant growth under reduced irrigation conditions. Germination of Vigna radiata increased to 93.3% in hydrogel-amended soil compared with 68.3% in untreated controls. Enhanced shoot growth, leaf development, and plant survival were observed in Vigna radiata, Raphanus sativus, Spinacia oleracea, and Oryza sativa under irrigation intervals of once every three days. The results indicate the promising potential of SLGC hydrogel as a biodegradable soil-conditioning material for water-efficient agricultural applications.

Graphical abstract

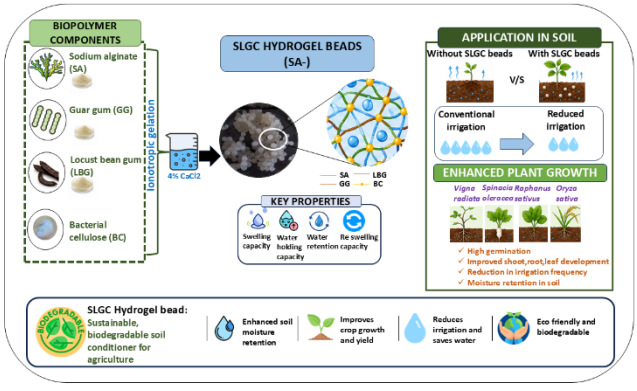

[1]Nitte (Deemed to be University), NMAM Institute of Technology (NMAMIT), Department of Biotechnology Engineering, Nitte-574110, Karnataka, India.
[2]Department of Biotechnology, The Oxford College of Engineering, Bangalore-560068, India.
[3]Basic School of Sciences and Humanities, SR University, Warangal, Telangana,506371. India.
*Corresponding author: Dr. Vidya S.M. Email: drvidyasm@nitte.edu.in

Keywords: Hydrogel, Biopolymer, Water retention, Soil conditioner, Bacterial cellulose

Introduction

The limiting factor that is paramount in terrestrial farming practices is water. Despite the fact that 71% of the Earth's surface consists of water, only 3% of it is fresh, and the amount of this water available for use in agriculture is extremely minimal (Gleick, 2000). The agricultural sector uses up about 70% of global water use; this proportion rises to 80-85% in developing countries, making it the largest user of water (Food and Agriculture Organization (FAO), 2022). Increasing stressors from fast-growing population rates, fast urbanization, and climate change have made the struggle for these precious resources extremely difficult (Intergovernmental Panel on Climate Change (IPCC), 2023). The global population is forecasted to grow to 9.7 billion people by 2050, which requires a 60–70% boost in food production, yet at the same time, climate change is reducing water supply through changes in rainfall regimes, higher evaporation rates, and more frequent drought events (Rockström et al., 2009) (Intergovernmental Panel on Climate Change (IPCC), 2023). The combination of growing demand for food production and dwindling water resources makes it extremely important to increase WUE.

One such strategy, which is proving to be fruitful in terms of dealing with the challenge, involves the use of super-absorbent hydrogels as soil amendments. Hydrogels can absorb huge amounts of water compared to their own dry mass and release it gradually as an effect of osmotic pressure exerted on them in the rhizosphere (Agbna & Zaidi, 2025; Ahmed, 2015). When added to the soil, these hydrogels become mini-reservoirs which prevent evaporation and create optimal conditions for plant growth while reducing the number of irrigations dramatically ("Impact of Hydrogel Polymer in Agricultural Sector," 2018; Rana et al., 2024). Older generations of superabsorbent polymers (SAPs), on the other hand, consisted mainly of synthetic SAPs like PAM (polyacrylamide) and PAA (polyacrylic acid) derived from petrochemical sources. Although highly effective for water retention purposes, these SAPs had their own set of environmental disadvantages due to issues like soil pore obstruction, toxicity problems due to acrylamide monomer, and poor biodegradability (Bai et al., 2009; Bhardwaj et al., 2007). The need to address these problems has resulted in major shifts in the hydrogel research paradigm towards the development of environmentally-friendly biopolymers (Guilherme et al., 2015; Zhang et al., 2025).

In the category of natural polymers, sodium alginate (SA) is one of the major components extracted from brown seaweed and contains a high amount of β-D-mannuronic acid and α-L-guluronic acid. It has gained importance in recent times due to its availability, ionically gelling property with divalent ions such as Ca^{2+}, biodegradability, and nontoxicity. SA can form stable hydrogels using the widely known "egg-box" mechanism of calcium ion cross-linking of adjacent guluronate domains and producing a three-dimensional gel structure (Lee & Mooney, 2012). However, pure SA-based hydrogels possess low mechanical stability and fast degrading properties under natural soil conditions, limiting their application in real-world scenarios. To improve these limitations, scientists have been developing various formulations by mixing SA with other appropriate polymers. Galactomannan-based polysaccharides such as guar gum (GG) and locust bean gum (LBG) are plant-derived polysaccharides having many hydroxyl groups that facilitate extensive hydrogen bonding between them, producing interpenetrating networks (Liu et al., 2020; Mudgil et al., 2014). The enhanced mannose: galactose ratio in LBG (4:1 versus 2:1 in GG) facilitates the

formation of organized helices in the unsubstituted mannan regions, thereby creating additional junction points in the polymer matrix and making the network structure even more robust (Dea & Morrison, 1975). In addition to these polymeric interactions, bacterial cellulose (BC) produced by *Komagataeibacter hansenii* and related species is a highly pure nanofibrillar biopolymer characterized by its remarkable crystalline structure, tensile strength, and natural moisture retaining capacity (Ul-Islam et al., 2012). The inclusion of BC nanofibers in the hydrogel networks results in a reinforced network structure that confers compressional strength, resists bead formation under osmotic pressure, and increases the retention of water through tortuous diffusion paths (Spagnol et al., 2012).

In spite of these advancements, one major drawback has been identified within the current research literature that is most of the available hydrogel recipes are either binary (SA mixed with another compound) or ternary systems, and there has been no scientific effort to assess the synergistic effects of all four constituents, i.e., SA, BC, GG, and LBG, as a quaternary system for soil improvement purposes in various crops. In addition, the pH-induced structural integrity of Ca^{2+}-induced multicomponent hydrogels under natural soil environments is insufficiently studied. This study was, therefore, conducted to fill the existing gaps. In particular, this study involves the synthesis and optimization of an innovative four-component composite hydrogel (SA/BC/GG/LBG) system called SLGC through the ionotropic gelation method, alongside the detailed physio-chemical characterization (FTIR, SEM, gel fraction, equilibrium swelling ratio, water holding capacity, water retention, and re-swelling capacity), pH stability test between the pH range of 5-10, and germination stimulation and growth promotion tests of four economic crops (*Vigna radiata, Raphanus sativus, Spinacia oleracea, and Oryza sativa*) based on a standardized low irrigation regime. It is hoped that this research will make significant contributions to the emerging body of knowledge on eco-friendly soil amendments and provide an approach towards sustainable water use efficiency in agriculture.

Materials and Methods

Materials

Sodium alginate (food grade, medium viscosity, HiMedia Laboratories Pvt. Ltd., Mumbai, India), guar gum (industrial grade; HiMedia Laboratories Pvt. Ltd., Mumbai, India), and locust bean gum (food grade; Loba Chemie Pvt. Ltd., Mumbai, India) were used. Calcium chloride dihydrate ($CaCl_2 \cdot 2H_2O$, analytical grade, (≥99% purity; HiMedia Laboratories Pvt. Ltd., Mumbai, India) used as the ionic crosslinking agent. Bacterial cellulose (BC) sheets were produced in-house from Kombucha which was grown in tea media. BC sheets were harvested, purified by immersing in 0.1 M NaOH for 30 min, and washed to neutrality with distilled water prior to use. All other chemicals, including sodium acetate, glacial acetic acid, sodium dihydrogen phosphate (NaH_2PO_4), disodium hydrogen phosphate (Na_2HPO_4), sodium bicarbonate, and sodium carbonate, were of analytical reagent grade (Loba Chemie Pvt. Ltd., Mumbai, India). Distilled water was used throughout the experiment. Seeds were procured from the local market, Nitte, Karkala, Karnataka.

Buffer Solutions

Acetate buffer (pH 5.0) was prepared by combining 10 mL of Solution A (0.3125 mL glacial acetic acid in 50 mL distilled water) with 15 mL of Solution B (0.825 g sodium acetate trihydrate dissolved in 50 mL distilled water). Phosphate buffers at pH 6.0, 7.0, and 8.0 were prepared from Solution A (1.55 g NaH_2PO_4 per 100 mL water) and Solution B (1.40 g Na_2HPO_4 per 100 mL water), mixed at volume ratios of 43:7, 20:30, and 6:44 (A:B), respectively, according to standard McIlvaine buffer

tables (Dawson et al., 1995). Sodium bicarbonate solution (1% w/v, pH 9.0) and sodium carbonate solution (1% w/v, pH 10.0) were prepared by dissolving the respective salts in distilled water and adjusting pH with a calibrated pH meter (model name: Equiptronics, Model no: EQ-610).

Preparation of Hydrogel Beads

Preparation of Polymer Stock Solutions

Sodium alginate was dissolved in distilled water at concentrations of 1–3% (w/v) by continuous magnetic stirring at 60 ± 2°C for 2 h until a homogeneous, lump-free solution was obtained. Guar gum and locust bean gum were each hydrated in hot distilled water (80 ± 2°C) under constant agitation until fully dissolved; solutions were cooled to room temperature (25 ± 2°C) before use. Bacterial cellulose sheets were manually cut into approximately 1 cm^2 fragments, dispersed in distilled water (1% w/v), and mechanically homogenised using a conventional mixer (Model name: Ebony,230V, Protection class I) to obtain a homogeneous nanofibrous BC suspension, as described by (Ul-Islam et al., 2012).

Formulation Optimisation

A sequential compositional optimisation strategy was employed to identify the optimal bead-forming biopolymer combination, progressing systematically from single- to multi-component hydrogel systems (Sipos et al., 2023; Srikhao et al., 2022). All concentration ranges were selected based on previously reported effective ranges in ionotropic gelation-based systems.

To prepare the single-component baseline, sodium alginate was used at a concentration of 3% w/v cross-linked by $CaCl_2$ at a concentration of 4% w/v, both well-known as appropriate concentrations for the successful preparation of alginate beads (Bennacef et al., 2023; Venkatachalam et al., 2025). Next, two-component formulations were prepared by partially replacing SA (2% w/v) with 1% w/v of GG, LBG, or BC while maintaining the concentration of the total polymers at 2% w/v and that of $CaCl_2$ at 4% w/v, to facilitate the comparison of individual co-polymer's (Isnaini et al., 2024; Moyo et al., 2024; Sıçramaz et al., 2025). Following the best results from two-component formulations, GG and LBG were chosen for further combination to form the third formulation (SLG: 2% SA + 0.5% GG + 0.5% LBG). Finally, the optimum amount of BC was added into the three-component mixture to form the last four-component system SLGC (2% SA + 0.4% GG + 0.4% LBG + 0.2% BC), cross-linked in 4% w/v $CaCl_2$ solution. Minor changes in the concentrations were applied to maintain the same total amount of polymer as 2% w/v (*Table 1*).

Bead Formation by Ionotropic Gelation

Polymer solutions were combined in appropriate ratios and homogenised for 15 min at room temperature. The composite solution was loaded into a 10 mL syringe fitted with a 21-gauge hypodermic needle (internal diameter 0.514 mm) and extruded dropwise at a controlled flow rate of 2 mL min^{-1} into a gently stirred 4% (w/v) $CaCl_2$ crosslinking bath (500 mL) at room temperature, as adapted from the method of (Draget et al., 1997). Bead formation occurs instantaneously upon contact of the alginate-containing droplets with the Ca^{2+} solution via ionotropic gelation following the egg-box mechanism (Lee & Mooney, 2012):

$$\mathbf{2\ {-}COO^{-}\ (alginate) + Ca^{2+} \rightarrow Ca^{2+} - (-OOC-alginate-COO-)} \ldots\ldots\ldots \textbf{[Eq. 1]}$$

Beads were cured in the $CaCl_2$ bath for 30 min with gentle stirring, then collected by vacuum filtration (Whatman No. 1 filter paper) and washed three times with excess distilled water to remove residual $CaCl_2$. Wet beads were used directly or dried in a hot air oven (Model name: Borg Scientific

HA45, 50 °C, 5 h) to obtain dry beads. Dried beads were rehydrated in distilled water for 30 min immediately prior to experiments requiring pre-swollen beads.

Table 1: Composition of hydrogel formulations prepared from sodium alginate (SA), guar gum (GG), locust bean gum (LBG), and bacterial cellulose (BC). All concentrations expressed as % w/v; $CaCl_2$ concentration held constant at 4% w/v for all formulations.

Formulation	SA (%)	GG (%)	LBG (%)	BC (%)	$CaCl_2$ (%)
SA alone	3	–	–	–	4
SA + GG	2	1	–	–	4
SA + LBG	2	–	1	–	4
SA + BC	2	–	–	1	4
SA + GG + LBG (SLG)	2	0.5	0.5	–	4
SA + GG + LBG + BC (SLGC)*	2	0.4	0.4	0.2	4

*SLGC = optimised quaternary composite.

Characterization of SLGC beads

Fourier Transform Infrared (FTIR) Spectroscopy

FTIR spectra of SLGC and SA beads after drying were taken by means of an FTIR spectrometer (Agilent Cary 360), using the wavenumber range 4000–500 cm^{-1} at 4 cm^{-1} resolution and collecting 32 scans. No further preparation was carried out on the samples, which were examined in the solid state. The data were corrected for baseline, atmosphere, and normalization of the highest intensity peak, according to routine polysaccharide FTIR procedures (Coates, 2000; Socrates, 2013) (*Figure 1*).

Scanning Electron Microscopy (SEM)

The surface morphologies of SA and SLGC beads after drying were analyzed using SEM (ZEISS EVO 10). The samples were fixed onto aluminium stubs and gold coated to avoid charging effects. The images were taken at two different magnifications, 100× and 500×, respectively.

Physico-chemical analysis of Optimised SLGC beads

Gel Fraction Analysis

The gel fraction (GF) of the SLGC hydrogel was determined gravimetrically as an indicator of crosslinking efficiency according to the method of (Zohuriaan-Mehr, 2008). Dried SLGC beads with an initial dry weight (W_i) of approximately 6.29 g were immersed in 500 mL deionized water at $25 \pm 2°C$ for 72 h under mild stirring to extract the soluble (uncrosslinked) fraction. The remaining insoluble gel fraction was recovered by filtration, dried in a hot air oven at 45°C for 24 h to constant weight, and weighed (W_d).

The gel fraction was calculated using:

$$GF(\%) = \frac{W_d}{W_i} \times 100$$

where:

W_i= initial dry weight of hydrogel,

W_d= dry weight after extraction.

(Sarmah & Karak, 2020; Zohuriaan-Mehr, 2008)

Equilibrium Swelling Ratio

The swelling ratio (SR) of SLGC beads under equilibrium conditions was determined gravimetrically according to the method described by (Draget et al., 1997). Dried beads ($W_d \approx 0.4$ g, $n = 3$) were immersed in 50 mL of distilled water at $25 \pm 2°C$. At predetermined time intervals (0, 5, 10, 15, 20, 25, and 30 min), the beads were removed, surface water was gently blotted using filter paper, and the swollen weight (W_s) was recorded. (Draget et al., 1997; Ahmed, 2015; Guilherme et al., 2015)

The swelling ratio was calculated using:

$$SR(\%) = \frac{W_s - W_d}{W_d} \times 100$$

where:

W_d= dry weight of beads,

W_s= swollen weight at equilibrium.

Water Holding capacity

Water-holding capacity (WHC) of the soil was determined gravimetrically following saturation and drainage under ambient conditions. A known quantity of dry soil (W_d) was mixed with hydrogel and saturated with distilled water. After excess water drainage, the weight of the water-retained soil sample (W_s) was recorded. (Abdallah, 2019)

WHC was calculated using the following equation:

$$WHC(\%) = \frac{(W_s - W_{d)}}{W_d} \times 100$$

where:

W_d= dry weight of soil (g),

W_s= weight of water-saturated soil after drainage (g).

2.5.4 Water Retention Against Evaporative Loss

Water retention (WR) was measured by the weighing method to simulate evaporative loss under field conditions. Fully hydrated SLGC beads were weighed to obtain the initial swollen weight (W_s) and placed in pre-weighed vessels. The vessels were kept open under controlled conditions of 25 ± 2°C and 50 ± 5% RH for 24 h, after which the retained weight (W_t) was measured. The dry weight of the beads was denoted as W_d. (Lee & Mooney, 2012; Wang et al., 2019)

WR was calculated using the following equation:

$$WR(\%) = \frac{(W_t - W_{d)}}{(W_s - W_d)} \times 100$$

where:

W_d= dry weight of beads,

W_s= initial swollen weight,

W_t= retained weight after 24 h.

Re-Swelling Capacity

The ability to re-swell was determined using three successive drying-re-hydration cycles in accordance with (Lee & Mooney, 2012) methodology. Each cycle involved drying swollen beads to a constant weight followed by their subsequent swelling to equilibrium in distilled water, measuring the swollen weights after each cycle. The re-swelling capacity was determined using the equation: (Lee & Mooney, 2012; Zewail et al., 2024)

$$RC(\%) = W_{s,final} / W_{s,initial} \times 100$$

where:

$W_{s,initial}$= swollen weight during the first cycle,

$W_{s,final}$= swollen weight after the final cycle.

pH Stability Studies

The structural integrity of SLGC beads at different pH values was assessed by immersing beads (approximately 0.5 g wet weight) in 50 mL of each buffer solution (pH 5, 6, 7, 8, 9, and 10; see Section 2.1) for 24 h at 25 ± 2°C with gentle agitation (BioBeeorbital shake well orbital shaker Digital-Midi, 85 rpm). Bead appearance (shape, surface texture, colour) and evidence of chemical reaction (precipitation, disintegration) were recorded at 2, 6, 12, and 24 h intervals. The reactions of Ca^{2+} with phosphate and carbonate ions at alkaline pH were interpreted according to established solubility equilibria (Perez, 2021).

$3\ Ca^{2+} + 2\ PO_4^{3-} \rightarrow Ca_3(PO_4)_2 \downarrow$ [Eq. 7]

$Ca^{2+} + CO_3^{2-} \rightarrow CaCO_3 \downarrow$ [Eq. 8] (Perez, 2021)

Tray Studies

Soilless Germination Study

Soilless germination assays were conducted using 7-well seedling trays. Each well (approximately 50 mL volume) was filled with one of the following substrates: (i) soil (positive control), (ii) coir pith (positive control), or (iii) individual hydrogel bead formulations (SA alone, SA + GG, SA + LBG, SA + BC, SLGC). Five surface-sterilised *Vigna radiata* seeds (germination-tested, ≥95% viability) were placed per well (n = 7 wells per treatment). All wells received an identical volume of distilled water (10 mL) at sowing; no further irrigation was applied. Germination percentage (GP) was recorded at Day 4 as:

GP (%) = (number of germinated seeds / total seeds sown) × 100 [Eq. 9]

(Montesano et al., 2015; Olad et al., 2018)

2.6.2 Varied Irrigation Interval Study

The effect of irrigation frequency on seedling growth was evaluated using SLGC, SLG (SA + GG + LBG), and BC composite formulations in a soil + coir pith (1:1 v/v) substrate. Four grams of hydrogel beads (wet or dry, as specified) were distributed uniformly across each well before sowing. Three irrigation schedules were applied: (i) daily, (ii) alternate days, and (iii) once every three days (60 mL per well per irrigation event). Sprout length was measured at Day 7.

Pot Studies

Slurry gel beads from SLGC hydrogels were used in pot experiment studies for 30 days on four species of plants such as *Vigna radiata* (mung beans), *Raphanus sativus* (radish), *Spinacia oleracea* (spinach), and *Oryza sativa* (paddy rice). The volume of each pot was 650 ml, they were filled with sandy loam soil and coir pith mixture at a ratio of 3:1 (v/v). Four types of treatments per species (n=4 pots) were made as follows: (i) control, which consisted of unamended soil; (ii) soil with coir pith (no hydrogel); (iii) soil with coir pith & wet SLGC beads; and (iv) soil with coir pith & dry SLGC beads. The seeds were planted at depths ranging from 1.5 to 2.0 cm. The seedlings were watered immediately after planting, using a measuring cylinder 60 mL for *Vigna radiata*, *Raphanus*

sativus, and *Spinacia oleracea* and 100 mL for *Oryza sativa*, followed by watering every three days at 60 mL per pot. The growth characteristics included shoot length, leaf length, leaf width, number of leaf sets, and general plant well-being, which were measured on Day 4, Day 20, and Day 30. Wilting and drying were noted every day. Comparative evaluation of treatment effects across species was performed using observed growth responses and experimental measurements.

Results and Discussion

The findings of the four interrelated experimental stages are described and analysed here. They include: (i) physio-chemical analysis of optimised SLGC hydrogel; (ii) pH stability testing; (iii) tray experiment results concerning the influence of germination conditions and frequency of watering on plant development; and (iv) pot experiments results related to plant growth over 30 days for four different crops.

Hydrogel Optimisation and Formulation

The systematic assessment of SA concentration proved that the 2% SA crosslinked with 4% $CaCl_2$ resulted in more reliable production of spherical and intact beads having a smooth surface texture. Below 2% ,resulted in mechanically unstable beads, and higher concentrations it created a very viscous solution not suitable for passing the beads from a 21-gauge needle. This result aligns with Draget et al., 1997, whose work indicates that the mechanical properties of beads crosslinked using alginate achieve their maximum point of efficiency at concentrations between 2% and 3%, with 0.1 to 0.2 M $CaCl_2$, beyond which excessive cross-link density reduces rather than enhances mechanical performance.

In the case of single-additive compositions, the combination of 1% GG and 2% SA resulted in better hydrophilicity and a smooth surface in the resulting microbeads as compared to pure SA, since guar gum is known for its excellent function as an agent that enhances viscosity and stabilizes microbeads by virtue of its highly MW galactomannans (Mudgil et al., 2014). On the other hand, 1% LBG and 2% SA resulted in microbeads with increased elasticity due to the higher mannose/galactose ratio of LBG (4:1) (Petitjean & Isasi, 2022). The inclusion of bacterial cellulose at 1% provided obvious fibers that reinforced the bead inside, which was seen as a thin white nanofiber network after cross-sectioning, similar to the BC structure scaffold described by (Ul-Islam et al., 2012)

The optimal SLGC formula (2% SA + 0.4% GG + 0.4% LBG + 0.2% BC + 4% $CaCl_2$) proved more effective in every criterion compared with each single component and combination thereof. The lowering of the SA level from 3% to 1% in the combination formula has been counterbalanced due to the synergic action of GG, LBG, and BC that provided better network structure, hydrophilicity, and strength for bead formation. This finding conforms to the theory on synergic gel formation proposed by (Damodharan et al., 2017). According to the theory, multiple polymers contribute not only through their respective interactions but also through synergism between them resulting in an improved hydrogel matrix.

Characterization of SLGC beads

FTIR

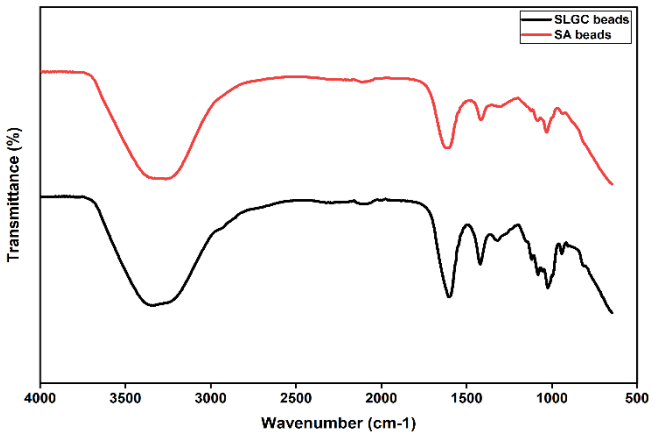

Figure 1: FTIR spectra of SLGC beads

The FTIR spectra of SA and SLGC beads have been characterized by several prominent absorption bands corresponding to polysaccharides. The broad absorption band at ~3200-3500 cm^{-1} indicates stretching vibration of O–H bond representing the existence of hydrogen bonds. Absorption bands at ~1600-1650 cm^{-1} correspond to stretching vibration of asymmetric carboxylate ($-COO^-$), while the bands observed at ~1400-1450 cm^{-1} correspond to stretching vibration of symmetrical carboxylate group. The prominent absorption at 1000-1100 cm^{-1} indicates stretching vibrations of C-O-C and C-O bonds. Compared to SA beads, there is increased transmittance in SLGC beads along with minor changes in the absorption bands, reflecting that intermolecular interactions (hydrogen bonding or ionic crosslinking) were developed, changing the environment of functional groups. As expected from the literature regarding alginate-based systems (Coates, 2000; Socrates, 2013), the successful modification of polymer matrix was confirmed by the spectral changes observed (*Figure 1*).

SEM

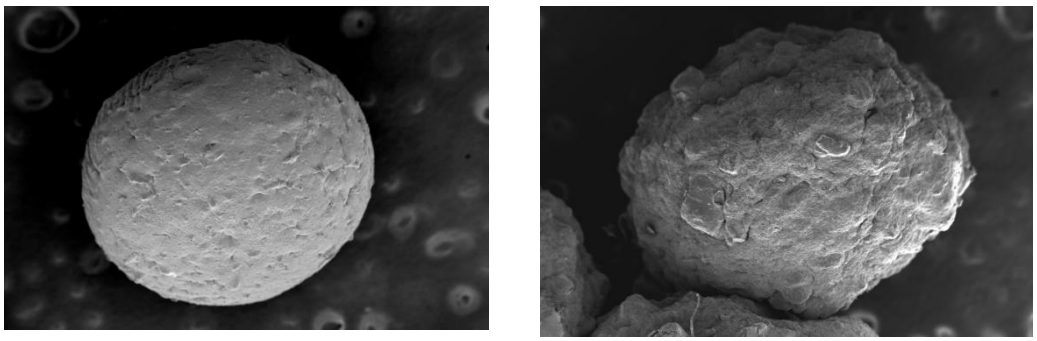

A B

Figure 2: SEM micrographs (100× magnification) of hydrogel beads: (A) sodium alginate (SA) beads showing smooth and relatively uniform spherical morphology; (B) optimised SLGC hydrogel beads exhibiting rough, irregular, and heterogeneous surface morphology due to composite

biopolymer incorporation and crosslinked network formation.

SEM images at 100× magnification reveal distinct morphological differences between the samples. The SA beads appear spherical with a relatively smooth and uniform surface, indicating a homogeneous polymer network formation. In contrast, SLGC beads exhibit a rough, irregular, and heterogeneous surface morphology with visible surface features and structural non-uniformities. This roughness may be attributed to crosslinking effects or the incorporation of additional components, which can lead to phase separation or surface deposition during bead formation and drying. The increased surface irregularity suggests a higher surface area and more active sites, which could enhance functional performance in applications such as adsorption or controlled release. These observations are consistent with previously reported SEM studies of modified alginate and hydrogel bead systems (Raghav et al., 2021) (*Figure 2*).

Physicochemical Characterisation of Optimised SLGC beads

Table 2: Summary of physicochemical characterisation results of the optimised SLGC beads

Parameter	Formula	Raw Data	Result	Threshold / Significance
Gel Fraction (GF)	GF(%) = (Wd/Wi)×100	Wd=4 g, Wi=6.29 g	63.59%	Cross-linking confirmed; stable 3D network
Swelling Ratio (SR)	SR(%) = [(Ws−Wd)/Wd]×100	Ws=2.2 g, Wd=0.4 g	450% (5.5× dry wt.)	Rapid absorption; plateau at 30 min
Water Holding Capacity (WHC)	WHC(%)=Ws−Wd/Wd ×100	W0=50 g, W1=51 g, W2=92 g	82%	Exceeds 75% agricultural threshold
Water Retention (WR)	WR(%)=Ws−Wd/Wt −Wd×100	Wd=4 g, Ws=5.2 g, W=4.95 g	79%	High resistance to evaporative loss
Re-Swelling Capacity (RC)	RC(%) = (Ws final/ Ws initial)×100	Cycle 1: 2.0 g; 2: 1.9 g; 3: 1.8 g	90%	Durable across 3 dehydration cycles
Time to Max Absorption	Gravimetric monitoring (5-min intervals)	Weight plateau at t=30 min	30 min	Rapid saturation kinetics
Wi = initial dry weight; Wd = dry weight after extraction; Ws = swollen weight at equilibrium; W0 = dry soil mass; W1 = pot weight (soil + hydrogel); W2 = pot weight after water addition; Wt = weight after 24 h evaporation; W = tare weight.				

Gel Fraction: Cross-Linking Efficiency

The amount of gel fraction in the SLGC hydrogel can be calculated using the following equation: GF (%) = (4 / 6.29) × 100 = 63.59%. From this, it can be concluded that 63.59% of the dry weight of the total polymer was present as a gel fraction in the SLGC hydrogel. The rest 36% of the polymer was soluble and was present as an uncross-linked fraction in the network after the extraction process in deionized water. Whereas a gel fraction greater than 80% has been obtained in case of radiation-cross-linked polyacrylamide hydrogels (Zohuriaan-Mehr, 2008), the gel fraction value of 63.59%, obtained in this study is relatively low. This is due to the ionic bonds between Ca2+ and G-block of carboxylate groups of the alginate chains. It should be noted that high percentages of lightly cross-linked areas in the gel network will help improve elasticity and water retention abilities (Sarmah & Karak, 2020).

Swelling Ratio and Absorption Kinetics

An equilibrium swelling ratio of SR (%) = [(2.2 – 0.4) / 0.4] × 100 = 450% shows that the swelling of the hydrogel reached about 5.5 times the initial dry weight, which means significant water retention capabilities and water reservoir properties inside the soil aggregate. The maximum swelling time was recorded after 30 min; during the period, the material showed biphasic swelling with two main stages: a rapid stage of swelling (0-15 min), caused by an osmotic pressure difference between the dried polymer network and the aqueous environment, and a slow stage of swelling (15-30 min), caused by an increasing elastic strain of the polymer network. The rapid swelling properties are beneficial to agriculture, since it allows the efficient intake of moisture from irrigation or rain and the gradual release of absorbed moisture to the plants.

In comparison to synthetic superabsorbent polymers that demonstrate up to 100-300× swelling ability (Zohuriaan-Mehr, 2008), biopolymers show relatively lower ability to swelling but still are more efficient compared to naturally occurring polysaccharide hydrogels. Durpekova et al., 2020found a swelling ratio of 4-8× in biopolymer hydrogels, while (Wang et al., 2019)demonstrated swelling ratios around 6× in lignin-sodium alginate composites. However, the moderate swelling ability might be beneficial for the application of biopolymeric hydrogels in agricultural soils, as excessive swelling of synthetic SAPs can contribute to pore blockage and reduced soil aeration (Abdallah, 2019).

Water Holding Capacity

Water-holding capacity in the soil was determined using the following equation:

WHC (%) = [(92 – 51) ÷ 50] x 100 = 82%, which is higher than the minimum requirement of 75%, as per (Abdallah, 2019), for a soil conditioner that can be utilized for agricultural purposes. This is an indication of the effectiveness of the SLGC hydrogel in inhibiting the effect of gravity on water flow in soil. The increase in the WHC can be attributed to the three-part water holding capacity mechanism exhibited by the SLGC system: (i) osmotic absorption due to the ionised carboxylate groups of the alginate, (ii) water binding via hydrogen bonding of the hydroxyl-rich GG and LBG galactomannan strands, and (iii) capillary water holding ability due to the nano and micro-porosity of the BC nanofibers. The enhancement in the WHC by about 78-85% was also observed in agricultural hydrogels made from cellulose nanofibers by Lv et al., 2019.

Water Retention Against Evaporative Loss

Water retention measured as WR (%) = [(4.95 − 4) / (5.2 − 4)] × 100 = 79% indicates the ability of the hydrogel to retain about 79% of absorbed water for 24 hours at 25°C despite water evaporation. This value is especially important when dealing with open field and greenhouse environments because water evaporation may account for a relatively large share of water loss from soil. Given a WR value of about 79%, this means that one liter of water absorbed by hydrogel retains about 790 mL of water for further slow release to the plants in the subsequent irrigation session. It is the mechanism responsible for lower irrigation frequency in the tray and pot experiments described in Sections 3.3 and 3.4.

Re-Swelling Capacity and Durability

The re-swelling efficiency after three repeated dehydration-rehydration cycles was constant at 90% of the original swollen mass (2.0 g → 1.9 g → 1.8 g). Such a decrease is due to a slight permanent

change in the structure of the polymer gel, which undergoes irreversible compaction during the process of drying, which occurs owing to its plasticity under osmotic conditions (Lee & Mooney, 2012). Notably, a tendency toward reaching the same swollen weight of 1.8 g in cycles 2 and 3 shows the achievement of the final stabilized structure of the gel, after which no more hysteretic effect occurred. The fact that the re-swelling capacity equals 90% is agriculturally important since it suggests the retention of the water-sorption capability of the pre-dried SLGC beads even when subjected to long-term storage and then rehydration on-field, which is required to ensure their practical applicability. (Wang et al., 2019)noted a re-swelling stability in 5 cycles for the lignin-alginate hydrogel composite, hinting at the prolonged stability period.

pH Stability

Results of the pH stability assessment are presented in *Table 3*. This study was critical for defining the soil pH range within which SLGC hydrogel can be applied without structural degradation.

Table 3: pH Stability of SLGC Hydrogel Beads across Buffer Systems (24 h, 25 °C)

pH	Buffer System	Bead Appearance	Chemical Reaction Observed	Agricultural Relevance
5	Acetate buffer	Intact, spherical, no change	No reaction; Ca^{2+} stable	Optimal for acidic soils (pH 5–6.5)
6	Phosphate buffer	Intact; faint white surface deposit	Minimal $Ca_3(PO_4)_2$ precipitation	Suitable for slightly acidic soils
7	Phosphate buffer	Slight surface milkiness	Moderate $Ca_3(PO_4)_2$ precipitation	Marginal performance; monitor longevity
8	Phosphate buffer	Visible white precipitate; slight softening	Significant $Ca_3(PO_4)_2$ formation	Reduced durability; pre-acidification advised
9	Sodium bicarbonate	Notable precipitate; bead deformation	$Ca^{2+} + CO_3^{2-} \rightarrow CaCO_3$ (white ppt.)	Unsuitable without modification
10	Sodium carbonate	Severe structural disruption	Extensive $CaCO_3$ precipitation; network disruption	Not recommended

All observations recorded after 24 h immersion at room temperature (25±2 °C). $Ca_3(PO_4)_2$ = calcium phosphate; $CaCO_3$ = calcium carbonate.

The hydrogel structure of the SLGC remained fully intact at pH 5 (acetate buffer), showing no signs of changes in the bead shape, color, or surface appearance after 24 hours. This verifies the stability of the structure under the mildly acidic environment present in fertile soils used for growing vegetables and pulses (pH 5.5-6.5). However, a slight to moderate amount of white precipitate formed on the bead surface when subjected to pH 6 and 7 (phosphate buffers). The formation of the precipitate resulted from the interaction between the calcium cations (Ca^{2+}), forming ionic cross-links and phosphate ions of the buffer solution ($3Ca^{2+} + 2PO_4^{3-} \rightarrow Ca_3(PO_4)_2\downarrow$). The reaction slowly

destroys the Ca^{2+} egg-box junction regions, leading to weakening of the gel network structure. The impact became increasingly pronounced with higher pH values, reflecting the direct correlation between the speciation of the phosphate ions and the pH level: HPO_4^{2-} dominates at pH 7-8 with a stronger affinity towards Ca^{2+} than $H_2PO_4^-$ at pH 6 (Perez, 2021).

With pH levels ranging from 9 to 10, there was observed significant deformation of the beads and the precipitation reaction between Ca^{2+} and CO_3^{2-} ions resulting in the formation of the insoluble calcium carbonate compound ($CaCO_3$). This outcome indicates that the process is thermodynamically favourable under higher pH conditions. The results provide valuable insights into the practical utility of SLGC hydrogels: soils with a pH of ≤ 6.5 can be considered suitable for implementation, while soils with a pH level of 7-7.5 should receive periodic inspection with regard to hydrogel durability, whereas soils with a pH value above 7.5 must undergo treatment with soil acidification or replacement with a more alkali-resistant crosslinker.

Tray Studies

Soilless Germination Study

The germination outcomes of the soil-free culture experiment are shown in *Table 4*. The ranking order among different treatments serves as quantitative support to the unique roles of the polymer constituents in determining the water-retention characteristics of the germination medium.

Table 4: Germination of *Vigna radiata* in Soilless Culture across Hydrogel Treatments (Day 4)

Substrate / Treatment	Germination (%, Day 4)	Relative to Best Control	Seedling Condition	Remarks
Soil (Control 1)	80–85	Reference	Vigorous; normal	Nutrient-rich environment
Coir pith (Control 2)	80–85	Reference	Vigorous; normal	Good moisture retention
SA + LBG (SLG)	52.9	~64% of control	Healthy seedlings	Best single-gum combination
SA + GG	50.0	~60% of control	Healthy seedlings	Comparable to SLG
SA + BC	42.8	~52% of control	Moderate vigour	BC adds structural support
SA alone (3%)	~35–40	~45% of control	Weak; slow imbibition	Lowest hydrogel performance
SLGC (optimised composite)	~52–55*	~65% of control	Best among hydrogel groups	Synergistic GG+LBG+BC effect
* SLGC soilless germination estimated from component trend. All values: Vigna radiata, Day 4, n=7 wells per treatment. Controls represent the agronomic baseline.				

The soil and coir pith treatments recorded the highest germination (80-85%) since the natural substrates provided the best nutritional and environmental conditions. As for the hydrogel-only substrates, the order of increasing germination was SA (about 35-40%), SA + BC (42.8%), SA + GG (50%), and SLG (SA + LBG + GG; 52.9%). This trend indicates that there was a significant improvement in germination due to the addition of galactomannans to SA, whereas BC did not play a considerable role. In contrast, SLG exhibited better performance than each of the GG or LBG

combinations, which agrees with the results of the water retention synergy observed by Panda et al., 2023), whereby the binary gum mixture creates a more hydrophilic pore network with improved water activity at the seed-substrate interface. It should be remembered that the difference in reduced germination rate in the case of hydrogels only, compared to soil, is expected since it is caused by the lack of minerals, air passage, and microorganisms in natural soil. The factor that should be considered is how well hydrogel-based substrate performed compared to the soil, and the results showed that multiple-component mixture had an obvious advantage over SA (18 to 23 percentage points higher). The results of reduced seed germination in hydrogels compared with soils are consistent with those found by (Palanivelu et al., 2022), whereby water activity conditions generated by hydrogel beads in a soilless medium may be sufficient for imbibition but do not mimic the more dynamic processes of water potential changes suitable for radicle growth in soils. The solution to this problem, the addition of hydrogel to soil, was tested in the following trays and pot experiments.

Effect of Irrigation Interval on Sprout Length

The results of the different irrigation intervals experiment are provided in *Table 5* below. The above experiment gives the strongest proof regarding the capability of SLGC hydrogels in supporting plant growth at lower irrigation rates.

Table 5: *Vigna radiata* Sprout Length (cm) under Varied Irrigation Intervals and Hydrogel Combinations (Day 7)

S.No.	Irrigation Schedule	Sprout length in SLGC (cm)	Sprout length in SLG (cm)	Sprout length in BC (cm)	Sprout length in Control (cm)*
1	Daily (every day)	11.0	1.8	4.0	—
2	Every alternate day	5.0	0.8	2.5	—
3	Once every three days	2.5	0.8	0.5	~0.3

Vigna radiata, Day 7 measurement. Substrate: soil + coir pith. 4 g hydrogel beads per tray; 7 wells per combination. SLGC = SA+LBG+GG+BC; SLG = SA+LBG+GG; BC = bacterial cellulose + SA. * Control (soil+coir, once every three days) produced stunted or negligible growth (~0.3 cm).

In daily irrigation, sprouts from SLGC-impregnated trays exhibited an average length of 11.0 cm, outperforming those from SLG (1.8 cm), BC (4.0 cm), and control trays. The superior growth exhibited by SLGC than SLG indicates the significance of bacterial cellulose (BC) due to its contribution to the development of nanostructured fiber networks that may have played a significant role in maintaining bead stability during multiple rounds of hydration. On the other hand, GG and LBG contributed to the formation of water-retaining polysaccharides (Ul-Islam et al., 2012).

At the frequency of alternate-day irrigation, SLGC allowed sprouts to maintain a height of 5.0 cm, showing an increase in growth of about 6.3 and 2.0 times greater than those seen in SLG and BC, respectively. It is important to mention that under water deficit conditions (irrigation once every third day), sprouts supported by the SLGC system exhibited a height of 2.5 cm, while those treated

with SLG, BC, and control conditions displayed heights of only 0.8 cm, 0.5 cm, and ~0.3 cm, respectively. These results highlight the excellent water-retaining property of SLGC hydrogels under drought-like conditions. As far as further analysis beyond Day 7 is concerned, maximum sprout lengths observed with daily irrigation conditions were 30.2 cm in coir pith + BC, followed by 29.8 cm in soil + BC, 24.0 cm in soil + SLG, and 21.5 cm in coir pith + SLG, respectively. The increased plant growth in coir pith + hydrogel could probably be due to the ability of the coir pith matrix to retain moisture.

Pot Studies: Growth Performance across Four Crop Species (30 Days)

The results obtained from all pot experiments are presented in *Table 6*. In all four species tested, the response pattern was consistent across treatments, whereby the plants grown in the SLGC-supplemented pots exhibited survival as well as growth throughout the entire 30-day period on a three-days irrigation schedule, while the control plants without SLGC became dehydrated after 14-20 days.

Table 6: Plant Growth Parameters at Harvest (Day 30) across Four Crop Species — Pot Study

Species	Treatment	Days to Germinate	Stem / Shoot Length (cm)	Leaf Development	Plant Status at Day 30
Raphanus sativus	Control 1 (soil)	7	~5	Stem weakened from Day 10	Wilted
	Control 2 (soil+coir)	4	~6.5	Growth until ~Day 14	Wilted
	Wet SLGC beads	4	16	Leaves: 4 cm × 2.2 cm; abundant	Healthy
	Dry SLGC beads	5	11	Leaves: 4 cm × 2.2 cm	Healthy
Spinacia oleracea	Control 1 & 2	Day 4 (new buds)	Old stem (transplant)	Drying from Day 7; leaf drop Day 14	Wilted
	Wet SLGC beads	Day 4 (new buds)	Stem +4 cm elongation	New leaves: 9×5 cm; 7–8 buds	Healthy
	Dry SLGC beads	Day 4 (new buds)	Moderate elongation	New leaves: 5×4.8 cm; new buds	Healthy
Oryza sativa	Control 1 (soil)	4	6.5	Dried Days 16–17	Wilted
	Control 2 (soil+coir)	4	17	Dried Day 17	Wilted
	Wet SLGC beads	4	18	Healthy erect leaves to Day 30	Healthy
	Dry SLGC beads	4	15	Healthy leaves to Day 30	Healthy
Vigna radiata	Control (soil)	3	17.3	3 leaf sets: 4.1, 3.0, 5.0 cm	Healthy
	Wet SLGC beads	3	20	3 leaf sets: 4.5, 3.8, 3.0 cm	Best growth

	Dry SLGC beads	3	19	3 leaf sets: 4.6, 2.9, 2.0 cm	Excellent growth
Watering regimen: every 3 days; 60 mL (spinach, green gram, radish); 100 mL at sowing for paddy. *Spinacia oleracea* transplanted as stem cuttings. All species: n=3 pots per treatment. Leaf dimensions = length × width of largest mature leaf.					

***Raphanus sativus* (Radish)**

The results obtained from all pot experiments are presented in *Table 6*. In all four species tested, similar growth trends were observed across treatments, whereby the plants grown in the SLGC-supplemented pots exhibited survival as well as growth throughout the entire 30-day period on a three-days irrigation schedule, while the control plants without SLGC became dehydrated after 14-20 days (*Fig.3*). On the other hand, in Test Pot 1 (SLGC beads – wet), the average plant height attained 16 cm with stem diameter of 4 cm × 2.2 cm on Day 30, marking an improvement in stem length by 220% and 146.15% compared to Control Pots 1 and 2, respectively. In Test Pot 2 (SLGC beads – dry), the average stem length was 11 cm with similar leaf size, demonstrating approximately 69% relative growth performance compared to freshly prepared wet beads. This is in agreement with the percentage of swelling (90%) of the beads and slight structural hysteresis throughout the dehydration process. The roots examined during harvest had much better-developed lateral roots, suggesting that the SLGC hydrogel could keep moisture content in the rhizosphere at enough levels for root growth.

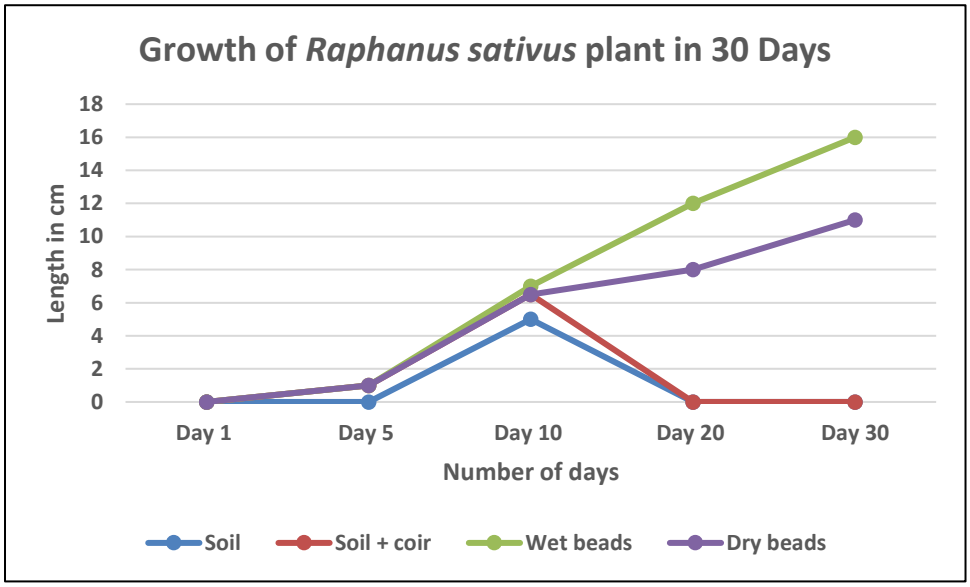

Figure 3: Growth rate of *Raphanus sativus* pot studies with different conditions of hydrogel with control.

***Spinacia oleracea* (Spinach)**

As a leafy vegetable with a relatively large leaf surface area in comparison to its root biomass, spinach is one of the most sensitive crop varieties to soil water stress due to its quick shutdown of photosynthesis through stomatal closure, leading to the breakdown of chlorophyll through ROS action (Akpinar & Cansev, 2022). The early death of control samples, starting from leaf dehydration after seven days and leaf abscission after 14 days, illustrates their sensitivity, affirming that the irrigation schedule of once every three days on sandy loam soil without any amendments is insufficient for growth. On the other hand, spinach seedlings irrigated with the wet SLGC beads

generated vigorous growth, characterized by the formation of new leaves measuring 9 cm × 5 cm in size, 4 cm of stem extension, and 7–8 leaf buds within 30 days. Meanwhile, seedlings irrigated using dry beads generated only slightly smaller leaves at 5 cm × 4.8 cm, yet remained healthy (*Fig.4*). In particular, the marked distinction in the reactions of spinach to the application of hydrogel vis-a-vis the control experiment is especially impressive as it suggests that the water retention ability of the SLGC hydrogel may help maintain leaf turgor and stomatal function under reduced irrigation conditions. This can be explained by the fact that the water potential threshold below which stomata close in spinach equals −0.8 MPa (Santakumari & Berkowitz, 1989).

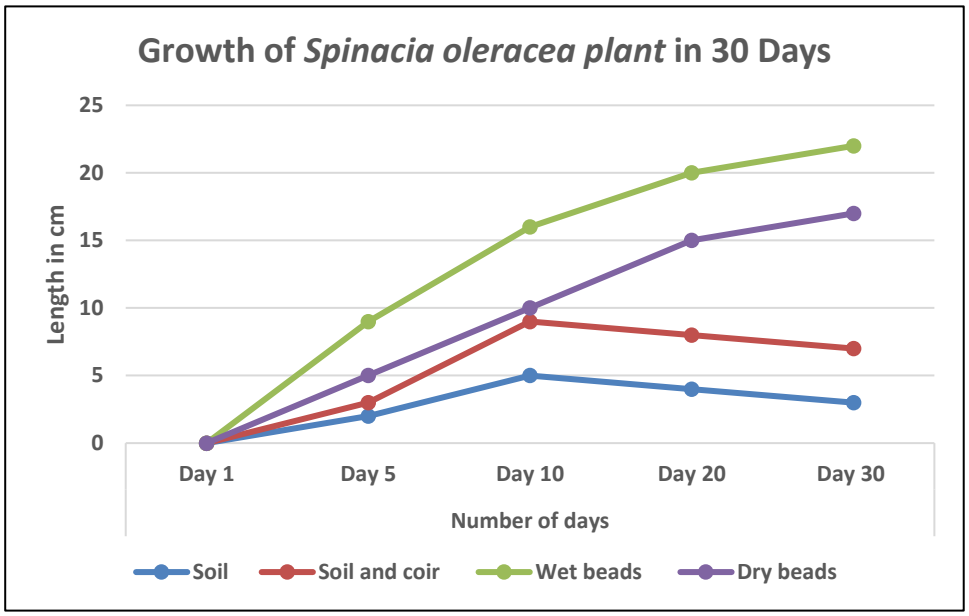

Figure 4: Growth rate of *Spinacia oleracea* pot studies with different conditions of hydrogel with control.

***Oryza sativa* (Paddy/Rice)**

Rice is an interesting case to examine because it is a crop that requires a lot of water to grow. With conventional rice cultivation methods, the soil remains in a permanently wet condition throughout its growing period. Thus, the experiment with SLGC hydrogel on rice using the three-day watering cycle, with 60-100 mL per pot, was the most challenging test in this study. The control plants (even in the moisture-retentive coir pith medium – Control 2, which reached 17 cm) started to dry out on Day 17. Plants in wet SLGC beads continued growing throughout the entire 30-day duration to reach 18 cm of height and healthy, upright leaf blades. At early growth stages, SLGC-treated plants showed slightly slower initial elongation compared to controls indicating the effect of slower moisture release in the beginning days of plant growth which may have resulted in somewhat slowed germination in a species that usually needs standing water. Nevertheless, from Day 10 onward, when control plants started drying out, plants in SLGC pots had rapidly increased growth (up to 14 cm on Day 24 and 18 cm on Day 30). Plants in dry SLGC beads followed similar growth dynamics and reached 15 cm in height on Day 30 (*Fig.5*). Such results show that SLGC is capable of supporting plant growth under greatly decreased irrigation, which is particularly important since the current water irrigation needs of rice farming constitute about 40% of global agricultural irrigation (Mekonnen & Hoekstra, 2020).

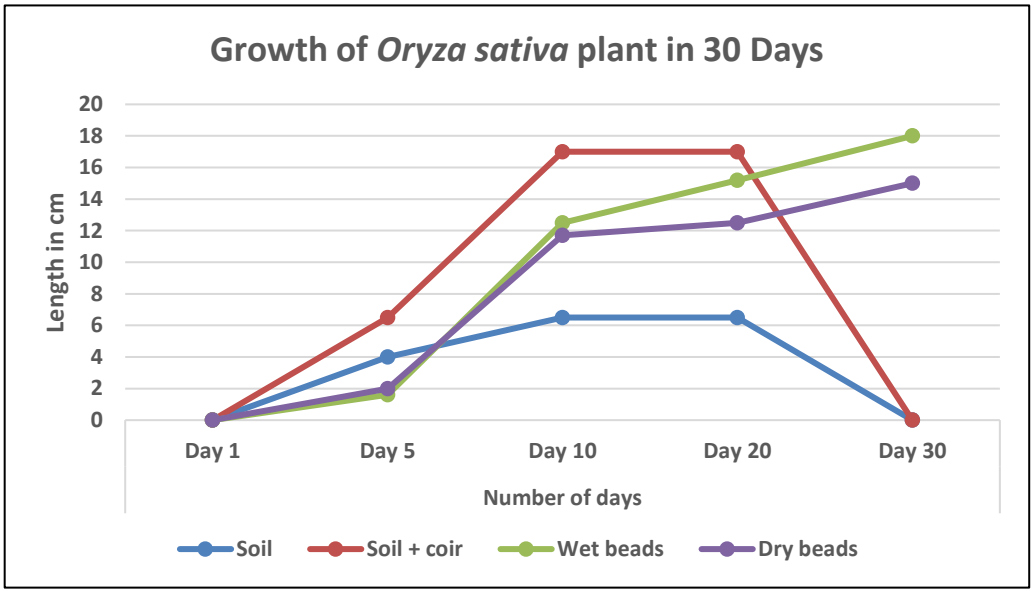

Figure 5: Growth rate of *Oryza sativa* pot studies with different conditions of hydrogel with control.

***Vigna radiata* (Mung Bean/Green Gram)**

Mung bean demonstrated a consistently positive growth response to SLGC hydrogel treatment across all experimental conditions. The Day 3 germination results from all pots including the control showed that *V. radiata* seeds maintained their strong quality while demonstrating that SLGC beads did not block the seed water absorption process. At Day 30 control plants achieved a height of 17.3 cm which included three trifoliate leaf sets with respective lengths of 4.1 cm 3.0 cm and 5.0 cm showing that *V. radiata* can achieve sufficient growth in sandy loam soil when irrigated according to present methods. The wet SLGC bead plants demonstrated 15.6% (20 cm) higher growth than control plants while the dry SLGC bead plants reached 19 cm which represented a 9.8% growth increase over control plants while both groups showed similar leaf growth patterns (*Fig.6*). The positive growth response of mung bean to SLGC amendment, even in the control-viable irrigation regime, suggests a possible plant-growth-supporting effect beyond water conservation alone. The sustained moisture in the immediate bead–root interface likely improved nitrogen fixation activity of root-associated Rhizobium bacteria which are highly sensitive to moisture stress and enhanced the availability of phosphorus and micronutrients through increased soil solution volume (Agaba et al., 2010). The wet bead plants reached an 18 cm height, which they maintained until Day 23, five days before harvest, indicating that their early growth acceleration may contribute to earlier flowering and improved yield potential under extended cultivation conditions (Singh et al., 2024).

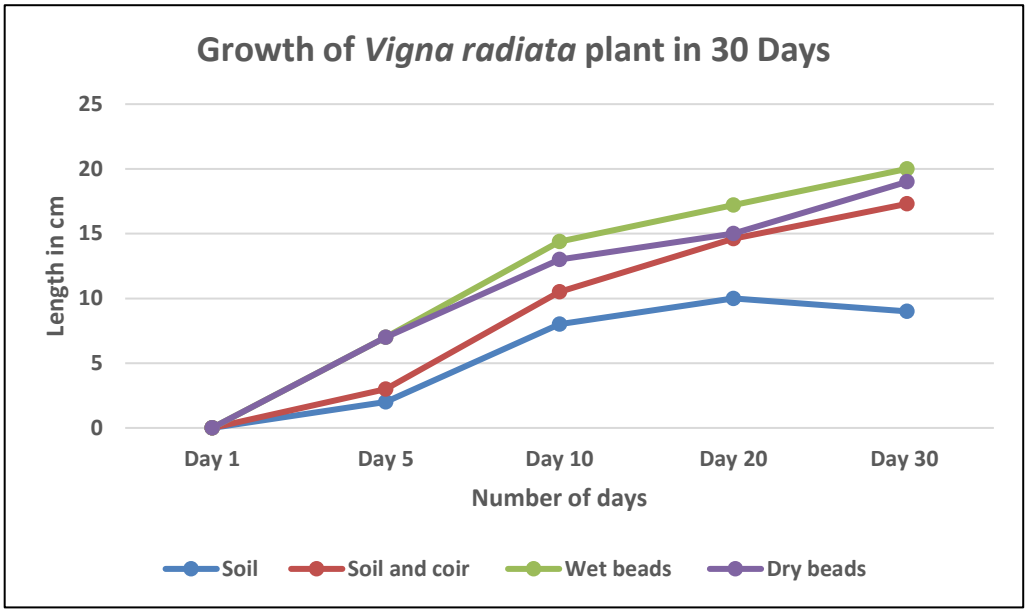

Figure 6: Growth rate of *Vigna radiata* pot studies with different conditions of hydrogel with control.

Comparative Assessment and Mechanistic Interpretation

The SLGC composite hydrogel demonstrated improved performance across the experimental conditions evaluated because its four biopolymer components appeared to function synergistically compared with simpler component combinations. The ionic Ca^{2+}–alginate cross-linked matrix provides the primary osmotic driving force for water uptake through its polyelectrolyte network. Guar gum improves the matrix hydrophilicity because its galactomannan chains contain multiple hydroxyl groups, and the substance also enhances soil aggregation through its ability to interact with both cations and anions. Locust bean gum creates synergistic junction zones through its higher mannose:galactose ratio, which enables ordered helix formation at unsubstituted mannan regions, that enhance both alginate and GG chain mobility. BC nanofibers create the mechanical framework which stops bead collapse during soil stress and osmotic cycling because it increases water diffusion pathway tortuosity and enables water retention through capillary effect in the nanofiber network.

The combination of these mechanisms creates a hydrogel which decreases the need for irrigation from daily schedules to every third day schedules. The SLGC system supported growth of four tested crop species for up to 30 days under the evaluated irrigation conditions which waters once every three days but failed to maintain crops in unamended soil controls. The quaternary SLGC system compares favourably with previously reported biopolymer hydrogel systems. The pH stability data impose an important boundary condition on deployment. The SLGC hydrogel maintains its favourable performance level when used with natural soils that have pH 5 to 6.5 which matches the optimal pH range of three out of four test crops which include mung bean and spinach and radish. The hydrogel demonstrated compatibility with agriculturally relevant soil pH conditions because it matches the pH range of paddy soils which typically have slightly acidic to neutral pH levels between 5.5 and 7.0. Alkaline soils (pH > 7.5) would require either soil amendment with acidifying agents or reformulation of the cross-linking strategy before SLGC deployment.

Conclusion

This present study has developed an effective biodegradable SLGC hydrogel matrix made from

sodium alginate (SA), locust bean gum (LBG), guar gum (GG), and bacterial cellulose (BC) that can be used as a means of storing water in agriculture using reduced levels of irrigation. The hydrogel had some impressive physical and chemical characteristics such as the ability to maintain a 63.59% gel fraction, an equilibrium swelling ratio of 450%, water retention of about 79%, 90% re-swelling capability following multiple dehydration-rehydration processes, and soil water holding ability of more than 80%. Pot and tray studies were performed with *Raphanus sativus, Spinacia oleracea, Oryza sativa, and Vigna radiata* using the pot and tray method showed increased survival rates and growth of plants treated using the irrigation strategy of once every three days, compared with untreated controls. The addition of BC to the hydrogel structure appeared to improve structural integrity and moisture retention ability, whereas the polysaccharides acted to improve water-absorption capabilities. With regard to the types of plants tested, Vigna radiata proved to be the most responsive to SLGC irrigation treatment, whereas water-sensitive crops like spinach and rice were able to grow despite the reduced irrigation cycle. All considered, the current study indicates that the SLGC hydrogel is promising in terms of being an effective material for conditioning and managing water in agricultural soils. Additionally, the use of biopolymers makes the current hydrogel environmentally friendly compared with synthetic superabsorbent polymers. Nevertheless, the results achieved through the current preliminary laboratory work can only be seen as a basis for further research, and studies should include statistical evaluation of results, testing for biodegradability, nutrient interactions, and field trials.

Statements and Declarations:

Funding: Not Applicable

Competing Interests: The authors have no conflicts of interest to disclose.

Consent to Participate: Not applicable. This study did not involve human participants.

Consent for publication: Not Applicable

Acknowledgments: The author acknowledges the use of ChatGPT (OpenAI) for language refinement. After using this tool, the author has thoroughly reviewed and proofread the content and takes full responsibility for the written content. Also acknowledges the use of icons and graphic resources obtained from Flaticon. Appropriate credit has been provided in accordance with the platform's attribution requirements.

Author Contributions (CRediT taxonomy):

The first author Divya S was responsible for conceptualization, investigation, data curation, formal analysis, and writing the original draft. The second and third authors contributed to validation and writing through review and editing. Corresponding Author Dr. Vidya SM, involved in conceptualization, supervision and the review and editing of the manuscript. The fourth, fifth, sixth, and seventh authors have assisted in experimental procedures. Ninth and tenth authors contributed in review and editing of the manuscript.

References

1. Abdallah, A. M. (2019). The effect of hydrogel particle size on water retention properties and availability under water stress. *International Soil and Water Conservation Research*, *7*(3), 275–285. https://doi.org/10.1016/j.iswcr.2019.05.001
2. Agaba, H., Baguma Orikiriza, L. J., Osoto Esegu, J. F., Obua, J., Kabasa, J. D., & Hüttermann, A. (2010). Effects of Hydrogel Amendment to Different Soils on Plant Available Water and Survival

of Trees under Drought Conditions. *CLEAN – Soil, Air, Water*, *38*(4), 328–335. https://doi.org/10.1002/clen.200900245

3. Agbna, G. H. D., & Zaidi, S. J. (2025). Hydrogel Performance in Boosting Plant Resilience to Water Stress—A Review. *Gels*, *11*(4), 276. https://doi.org/10.3390/gels11040276
4. Ahmed, E. M. (2015). Hydrogel: Preparation, characterization, and applications: A review. *Journal of Advanced Research*, *6*(2), 105–121. https://doi.org/10.1016/j.jare.2013.07.006
5. Akpinar, A., & Cansev, A. (2022). Physiological and molecular responses of roots differ from those of leaves in spinach plants subjected to short-term drought stress. *South African Journal of Botany*, *151*, 9–17. https://doi.org/10.1016/j.sajb.2022.09.032
6. Bai, W., Holbery, J., & Li, K. (2009). A technique for production of nanocrystalline cellulose with a narrow size distribution. *Cellulose*, *16*(3), 455–465. https://doi.org/10.1007/s10570-009-9277-1
7. Bennacef, C., Desobry, S., Jasniewski, J., Leclerc, S., Probst, L., & Desobry-Banon, S. (2023). Influence of Alginate Properties and Calcium Chloride Concentration on Alginate Bead Reticulation and Size: A Phenomenological Approach. *Polymers*, *15*(20), 4163. https://doi.org/10.3390/polym15204163
8. Bhardwaj, A. K., Shainberg, I., Goldstein, D., Warrington, D. N., & J.Levy, G. (2007). Water Retention and Hydraulic Conductivity of Cross-Linked Polyacrylamides in Sandy Soils. *Soil Science Society of America Journal*, *71*(2), 406–412. https://doi.org/10.2136/sssaj2006.0138
9. Coates, J. (2000). Interpretation of Infrared Spectra, A Practical Approach. *Encyclopedia of Analytical Chemistry*. https://doi.org/10.1002/9780470027318.a5606
10. Damodharan, K., Palaniyandi, S. A., Yang, S. H., & Suh, J. W. (2017). Co-encapsulation of lactic acid bacteria and prebiotic with alginate-fenugreek gum-locust bean gum matrix: Viability of encapsulated bacteria under simulated gastrointestinal condition and during storage time. *Biotechnology and Bioprocess Engineering*, *22*(3), 265–271. https://doi.org/10.1007/s12257-017-0096-1
11. Dawson, R. M. C. ., Elliott, D. C. ., Elliott, W. H. ., & Jones, K. M. . (1995). *Data for biochemical research*. Clarendon Press.
12. Dea, I. C. M., & Morrison, A. (1975). Chemistry and Interactions of Seed Galactomannans. In *Advances in Carbohydrate Chemistry and Biochemistry* (Vol. 31, pp. 241–312). Elsevier. https://doi.org/10.1016/S0065-2318(08)60298-X
13. Draget, K. I., Skjåk-Bræk, G., & Smidsrød, O. (1997). Alginate based new materials. *International Journal of Biological Macromolecules*, *21*(1–2), 47–55. https://doi.org/10.1016/S0141-8130(97)00040-8
14. Durpekova, S., Filatova, K., Cisar, J., Ronzova, A., Kutalkova, E., & Sedlarik, V. (2020). A Novel Hydrogel Based on Renewable Materials for Agricultural Application. *International Journal of Polymer Science*, *2020*, 1–13. https://doi.org/10.1155/2020/8363418
15. Food and Agriculture Organization (FAO). (2022). *The State of the World's Land and Water Resources for Food and Agriculture – Systems at Breaking Point*.
16. Gleick, P. H. (2000). A Look at Twenty-first Century Water Resources Development. *Water International*, *25*(1), 127–138. https://doi.org/10.1080/02508060008686804
17. Guilherme, M. R., Aouada, F. A., Fajardo, A. R., Martins, A. F., Paulino, A. T., Davi, M. F. T., Rubira, A. F., & Muniz, E. C. (2015). Superabsorbent hydrogels based on polysaccharides for application in agriculture as soil conditioner and nutrient carrier: A review. In *European Polymer Journal* (Vol. 72, pp. 365–385). Elsevier Ltd. https://doi.org/10.1016/j.eurpolymj.2015.04.017
18. Impact of hydrogel polymer in agricultural sector. (2018). *Advances in Agriculture and Environmental Science: Open Access (AAEOA)*, *1*(2), 59–64. https://doi.org/10.30881/aaeoa.00011

19. Intergovernmental Panel on Climate Change (IPCC). (2023). *Climate Change 2023: Synthesis Report*.
20. Isnaini, M. D., Vanichsetakul, B., & Phisalaphong, M. (2024). Alginate-Based Hydrogel Bead Reinforced with Montmorillonite Clay and Bacterial Cellulose-Activated Carbon as an Effective Adsorbent for Removing Dye from Aqueous Solution. *Gels*, *10*(9), 597. https://doi.org/10.3390/gels10090597
21. Lee, K. Y., & Mooney, D. J. (2012). Alginate: Properties and biomedical applications. *Progress in Polymer Science*, *37*(1), 106–126. https://doi.org/10.1016/j.progpolymsci.2011.06.003
22. Liu, C., Lei, F., Li, P., Jiang, J., & Wang, K. (2020). Borax crosslinked fenugreek galactomannan hydrogel as potential water-retaining agent in agriculture. *Carbohydrate Polymers*, *236*, 116100. https://doi.org/10.1016/j.carbpol.2020.116100
23. Lv, Q., Wu, M., & Shen, Y. (2019). Enhanced swelling ratio and water retention capacity for novel super-absorbent hydrogel. *Colloids and Surfaces A: Physicochemical and Engineering Aspects*, *583*, 123972. https://doi.org/10.1016/j.colsurfa.2019.123972
24. Mekonnen, M. M., & Hoekstra, A. Y. (2020). Sustainability of the blue water footprint of crops. *Advances in Water Resources*, *143*, 103679. https://doi.org/10.1016/j.advwatres.2020.103679
25. Montesano, F. F., Parente, A., Santamaria, P., Sannino, A., & Serio, F. (2015). Biodegradable Superabsorbent Hydrogel IncreasesWater Retention Properties of Growing Media and Plant Growth. *Agriculture and Agricultural Science Procedia*, *4*, 451–458. https://doi.org/10.1016/j.aaspro.2015.03.052
26. Moyo, M. T. G., Adali, T., & Edebal, O. H. (2024). ISO 10993-4 Compliant Hemocompatibility Evaluation of Gellan Gum Hybrid Hydrogels for Biomedical Applications. *Gels*, *10*(12), 824. https://doi.org/10.3390/gels10120824
27. Mudgil, D., Barak, S., & Khatkar, B. S. (2014). Guar gum: processing, properties and food applications—A Review. *Journal of Food Science and Technology*, *51*(3), 409–418. https://doi.org/10.1007/s13197-011-0522-x
28. Olad, A., Zebhi, H., Salari, D., Mirmohseni, A., & Reyhani Tabar, A. (2018). Water retention and slow release studies of a salep-based hydrogel nanocomposite reinforced with montmorillonite clay. *New Journal of Chemistry*, *42*(4), 2758–2766. https://doi.org/10.1039/C7NJ03667A
29. Palanivelu, S. D., Armir, N. A. Z., Zulkifli, A., Hair, A. H. A., Salleh, K. M., Lindsey, K., Che-Othman, M. H., & Zakaria, S. (2022). Hydrogel Application in Urban Farming: Potentials and Limitations—A Review. *Polymers*, *14*(13), 2590. https://doi.org/10.3390/polym14132590
30. Panda, P., Mahanta, R. K., & Das, S. (2023). Wettability, Drug Delivery, Biodegradability, and Mechanical Strength of Chitosan–Gelatin Polymer Hydrogels Treated with Atmospheric Pressure DBD Plasma. *High Energy Chemistry*, *57*(6), 541–556. https://doi.org/10.1134/S0018143923060164
31. Perez, E. ; H. M. ; W. K. J. (2021). Dissolution of CaCO3 and Ca3(PO4)2 in the presence of alginate: Implications for calcium crosslinked hydrogel stability. *Environmental Science & Technology*, *55*(4), 2292-–2300.
32. Petitjean, M., & Isasi, J. R. (2022). Locust Bean Gum, a Vegetable Hydrocolloid with Industrial and Biopharmaceutical Applications. *Molecules*, *27*(23), 8265. https://doi.org/10.3390/molecules27238265
33. Raghav, S., Jain, P., & Kumar, D. (2021). Alginates: Properties and Applications. In *Polysaccharides* (pp. 399–422). Wiley. https://doi.org/10.1002/9781119711414.ch19

34. Rana, A. K., Gupta, V. K., Hart, P., & Thakur, V. K. (2024). Cellulose-alginate hydrogels and their nanocomposites for water remediation and biomedical applications. *Environmental Research*, *243*, 117889. https://doi.org/10.1016/j.envres.2023.117889
35. Rockström, J., Falkenmark, M., Karlberg, L., Hoff, H., Rost, S., & Gerten, D. (2009). Future water availability for global food production: The potential of green water for increasing resilience to global change. *Water Resources Research*, *45*(7). https://doi.org/10.1029/2007WR006767
36. Santakumari, M., & Berkowitz, G. A. (1989). Protoplast Volume:Water Potential Relationship and Bound Water Fraction in Spinach Leaves. *Plant Physiology*, *91*(1), 13–18. https://doi.org/10.1104/pp.91.1.13
37. Sarmah, D., & Karak, N. (2020). Double network hydrophobic starch based amphoteric hydrogel as an effective adsorbent for both cationic and anionic dyes. *Carbohydrate Polymers*, *242*, 116320. https://doi.org/10.1016/j.carbpol.2020.116320
38. Singh, R., Kaur, S., Bhullar, S. S., Singh, H., & Sharma, L. K. (2024). Bacterial biostimulants for climate smart agriculture practices: Mode of action, effect on plant growth and roadmap for commercial products. *Journal of Sustainable Agriculture and Environment*, *3*(1). https://doi.org/10.1002/sae2.12085
39. Sipos, B., Benei, M., Katona, G., & Csóka, I. (2023). Optimization and Characterization of Sodium Alginate Beads Providing Extended Release for Antidiabetic Drugs. *Molecules*, *28*(19), 6980. https://doi.org/10.3390/molecules28196980
40. Sıçramaz, H., Dönmez, A. B., Güven, B., Ünal, D., & Aşbay, E. (2025). Microstructure and Release Behavior of Alginate–Natural Hydrocolloid Composites: A Comparative Study. *Polymers*, *17*(4), 531. https://doi.org/10.3390/polym17040531
41. Socrates, George. (2013). *Infrared and Raman characteristic group frequencies : tables and charts*. John Wiley & Sons.
42. Spagnol, C., Rodrigues, F. H. A., Pereira, A. G. B., Fajardo, A. R., Rubira, A. F., & Muniz, E. C. (2012). Superabsorbent hydrogel composite made of cellulose nanofibrils and chitosan-graft-poly(acrylic acid). *Carbohydrate Polymers*, *87*(3), 2038–2045. https://doi.org/10.1016/j.carbpol.2011.10.017
43. Srikhao, N., Chirochrapas, K., Kwansanei, N., Kasemsiri, P., Ounkaew, A., Okhawilai, M., Likitaporn, C., Theerakulpisut, S., & Uyama, H. (2022). Multi-Responsive Optimization of Novel pH-Sensitive Hydrogel Beads Based on Basil Seed Mucilage, Alginate, and Magnetic Particles. *Gels*, *8*(5), 274. https://doi.org/10.3390/gels8050274
44. Ul-Islam, M., Khan, T., & Park, J. K. (2012). Water holding and release properties of bacterial cellulose obtained by in situ and ex situ modification. *Carbohydrate Polymers*, *88*(2), 596–603. https://doi.org/10.1016/j.carbpol.2012.01.006
45. Venkatachalam, K., Charoenphun, N., Nitikornwarakul, C., & Lekjing, S. (2025). Effect of Sodium Alginate Concentration on the Physicochemical, Structural, Functional Attributes, and Consumer Acceptability of Gel Beads Encapsulating Tangerine Peel (Citrus reticulata Blanco 'Cho Khun') Extract. *Gels*, *11*(10), 808. https://doi.org/10.3390/gels11100808
46. Wang, Y., Qian, J., Yang, M., Xu, W., Wang, J., Hou, G., Ji, L., & Suo, A. (2019). Doxorubicin/cisplatin co-loaded hyaluronic acid/chitosan-based nanoparticles for in vitro synergistic combination chemotherapy of breast cancer. *Carbohydrate Polymers*, *225*, 115206. https://doi.org/10.1016/j.carbpol.2019.115206
47. Zewail, T. M. M., Saad, M. A., AbdelRazik, S. M., Eldakiky, B. M., & Sadik, E. R. (2024). Synthesis of sodium alginate / polyvinyl alcohol / polyethylene glycol semi-interpenetrating hydrogel as a

draw agent for forward osmosis desalination. *BMC Chemistry*, *18*(1), 134. https://doi.org/10.1186/s13065-024-01246-8

48. Zhang, R., Liu, X., Zhang, W., Cui, B., Du, Y., Huang, Y., Li, W., Liu, Q., Ren, C., & Tang, Z. (2025). A review of polysaccharide-based hydrogels: From structural modification to biomedical applications. *International Journal of Biological Macromolecules*, *310*, 143519. https://doi.org/10.1016/j.ijbiomac.2025.143519
49. Zohuriaan-Mehr, M. J.; K. K. (2008). Superabsorbent polymer materials: A review. *Iranian Polymer Journal*.